New Journal of Chemistry

Supporting Information

Multi-responsive luminescent sensor based on three dimensional lanthanide metal–organic framework

Yufang Tao,[a] Ping Zhang,[a] Junning Liu,[b] Xiaodong Chen,[a] Xiuli Guo,[a] Haoqing Jin,[a] Juan Chai,[a] Li Wang*[a] and Yong Fan*[a]

Table of Contents

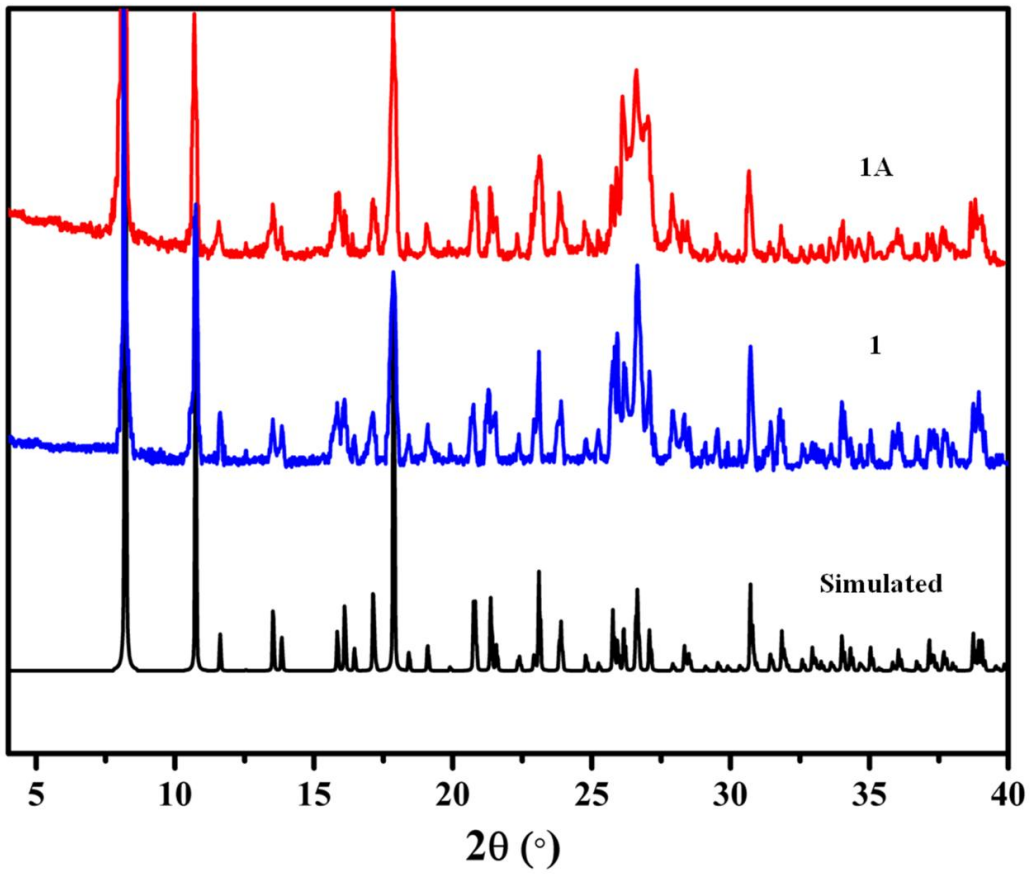

Fig. S1 Powder X-ray diffraction patterns of **1** and **1A** (activated product of **1**).

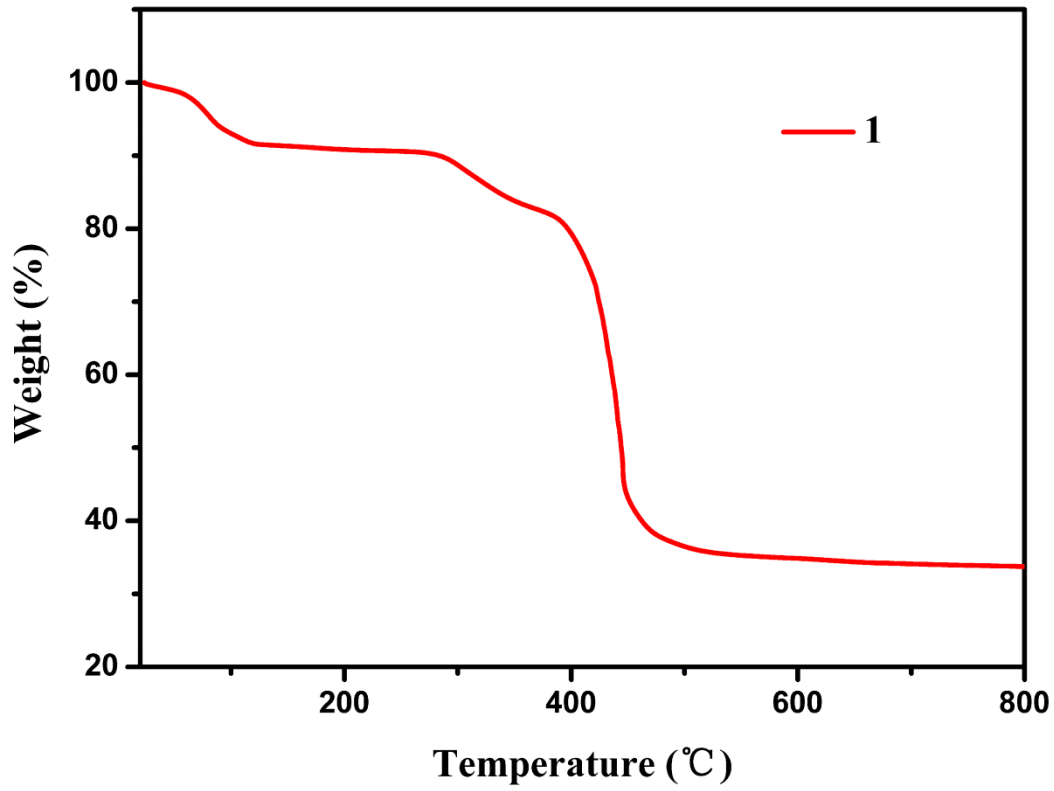

Fig. S2 TGA curve of **1** measured in air atmosphere.

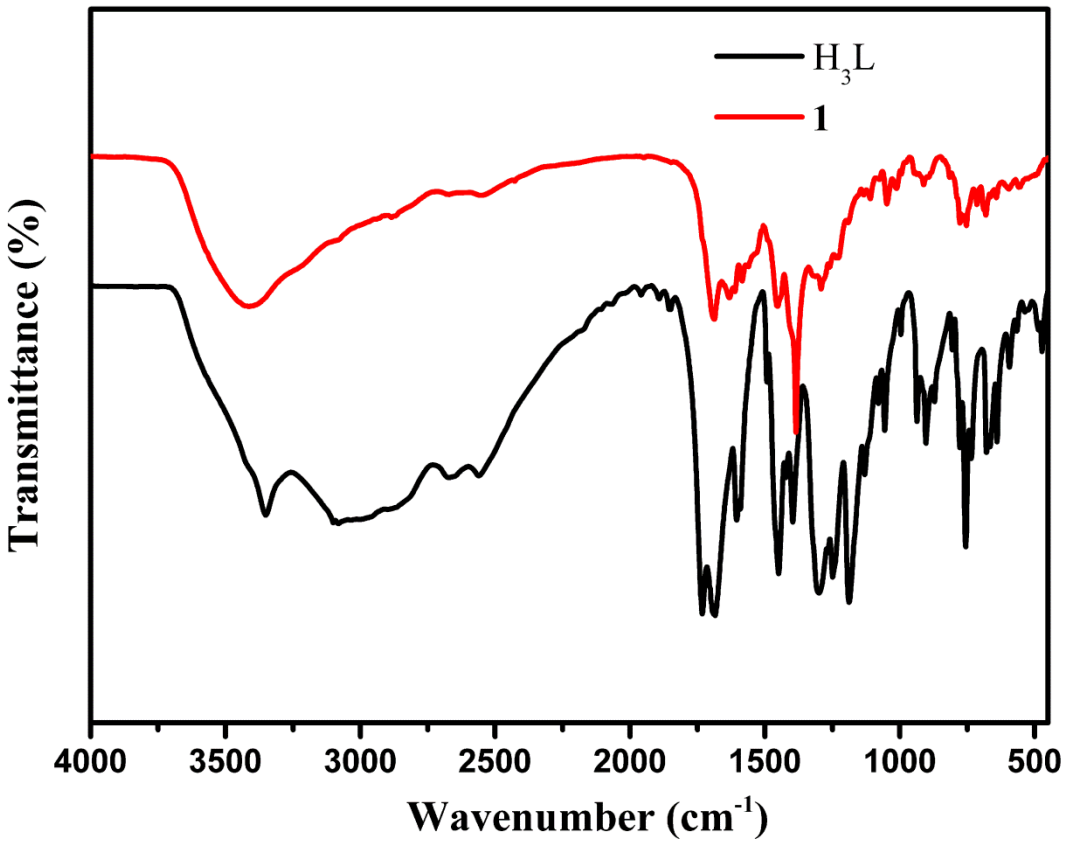

Fig. S3 IR spectra of H_3L ligand and **1**.

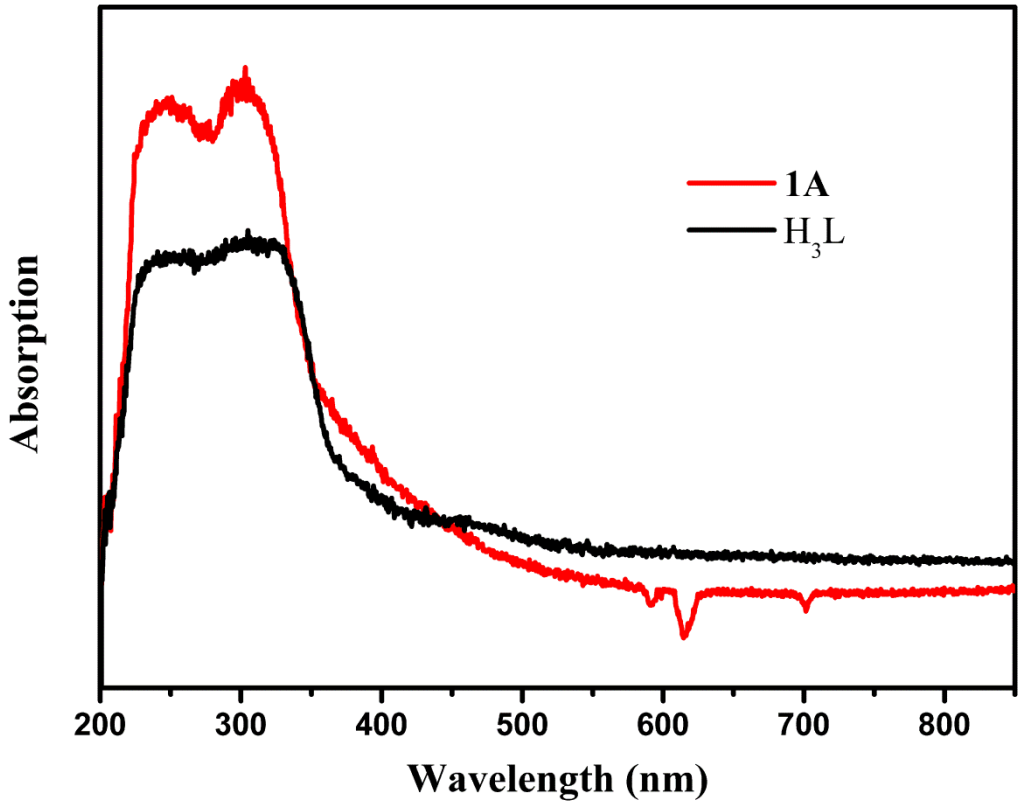

Fig. S4 The UV-vis absorption spectra of free H_3L ligand and **1A** at room temperature.

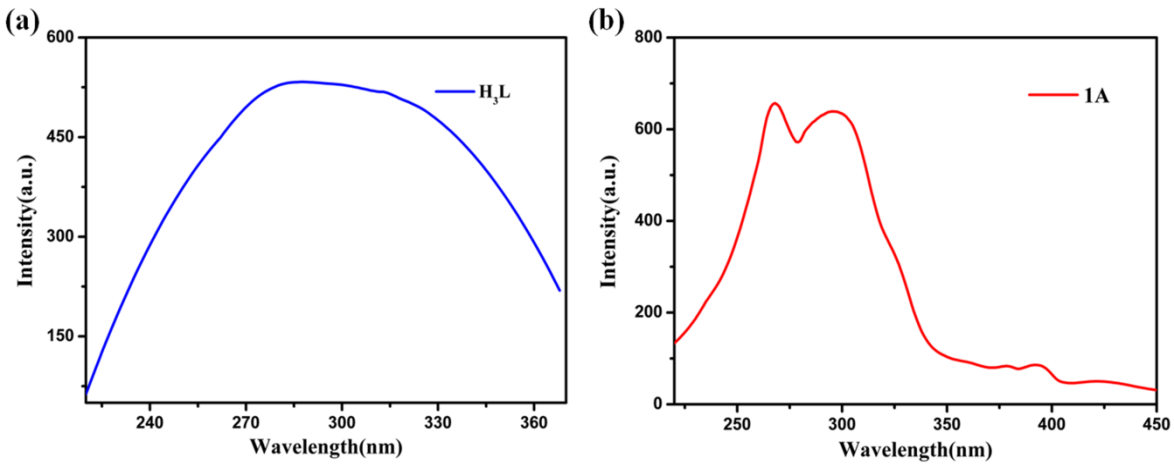

Fig. S5 Solid-state excitation spectra of H_3L ligand and **1A** at room temperature.

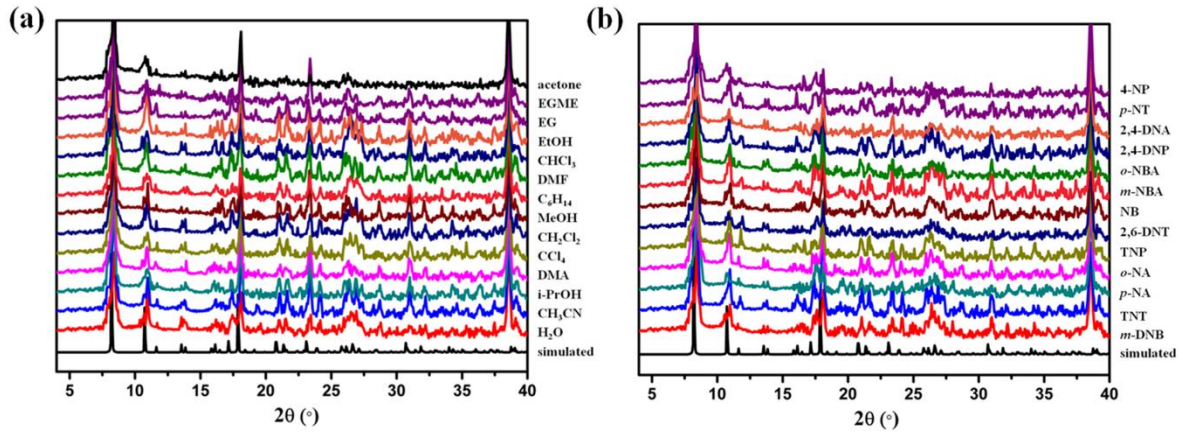

Fig. S6 The powder X-ray diffractions of **1A** after sensing organic solvents (a) and nitro explosives (b).

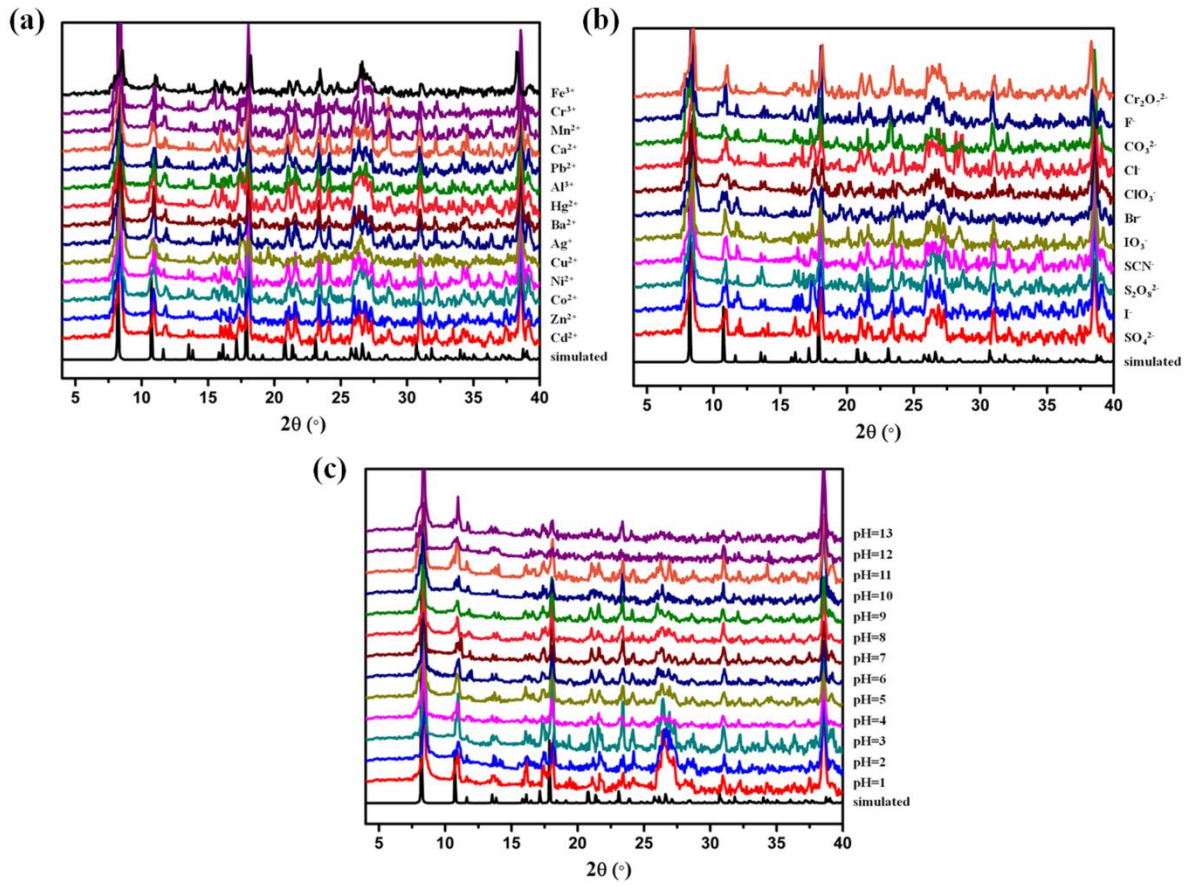

Fig. S7 The powder X-ray diffractions of **1A** after sensing cations (a), anions (b) and pH (c) in aqueous solution.

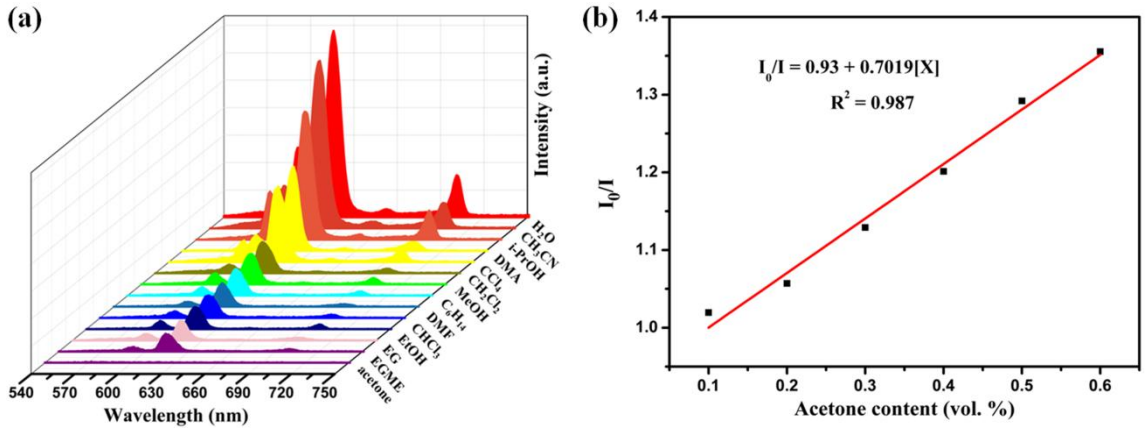

Fig. S8 (a) Luminescence spectra of **1A** treated with different solvents. (b) The Stern–Völmer (SV) quenching curve for **1A** in aqueous solutions of different concentrations of acetone.

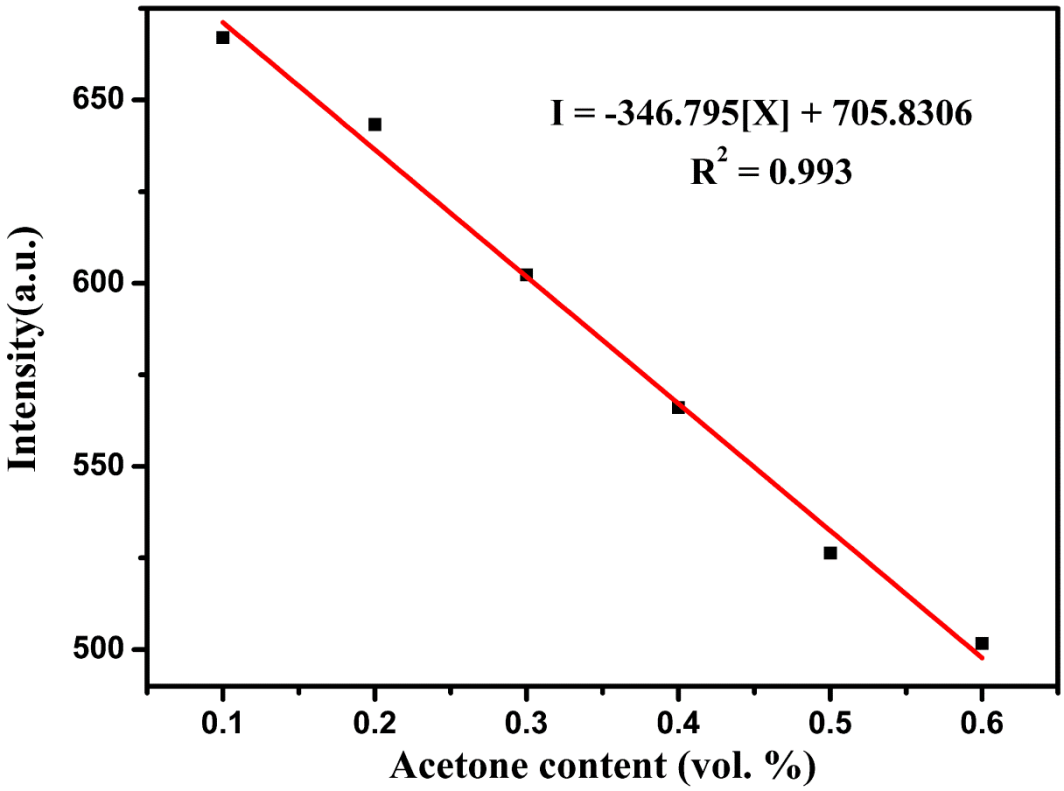

Fig. S9 Relation of luminescence intensity against acetone added into **1A** suspension and their linear fitting curve for the estimation of LOD.

Detection Limit = 3σ/*k*

= (3 ×8.1379)/ 346.795

= 0.0704 vol%

Multiple number of luminescence spectra (n = 10) were recorded for the blank sample of **1A** suspension. Sample standard deviation σ for the blank probe without the addition of acetone was calculated to be 8.1379.

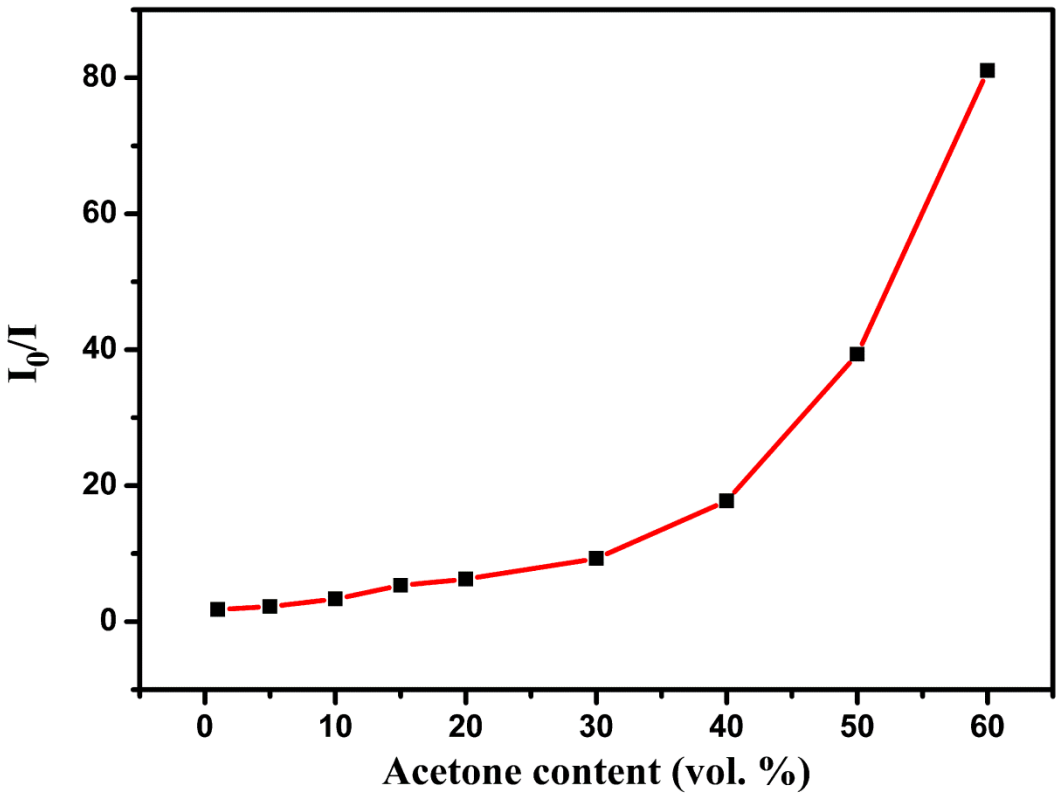

Fig. S10 Stern–Völmer plot for the luminescence intensities of **1A** in aqueous solutions of different concentrations of acetone.

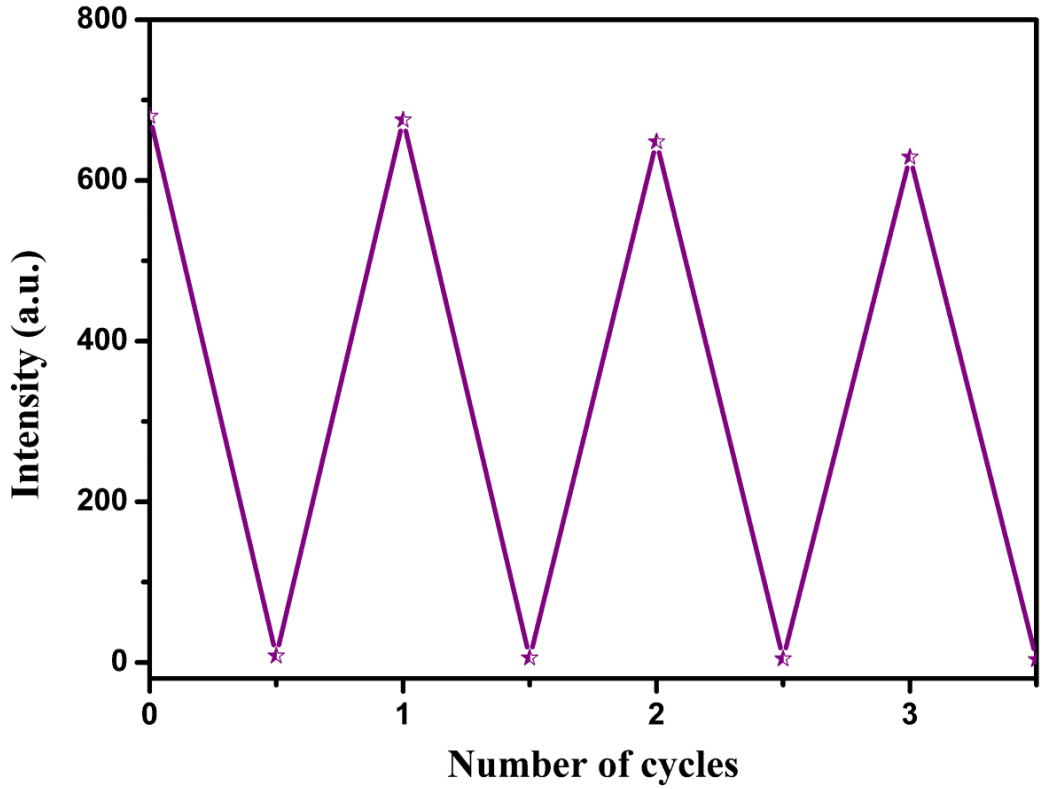

Fig. S11 Cyclic response of **1A** for detecting acetone (luminescence intensity at 616 nm).

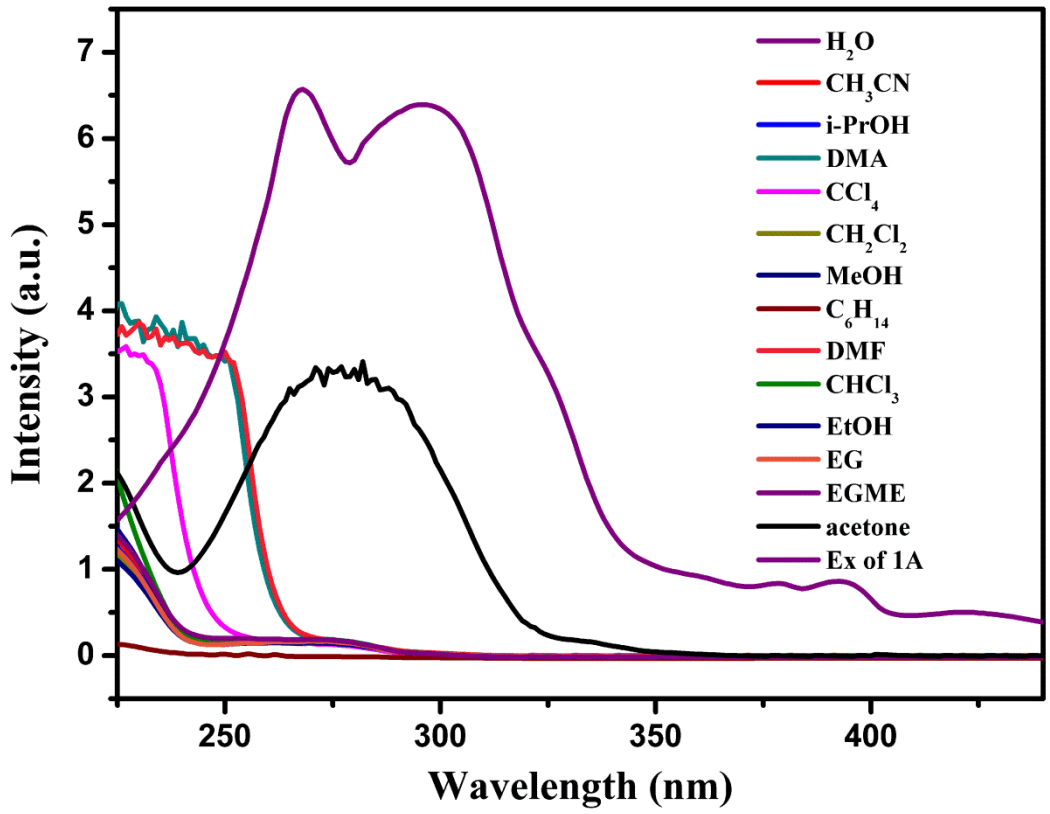

Fig. S12 The absorption spectra of different organic solvents and the excitation spectrum of **1A**.

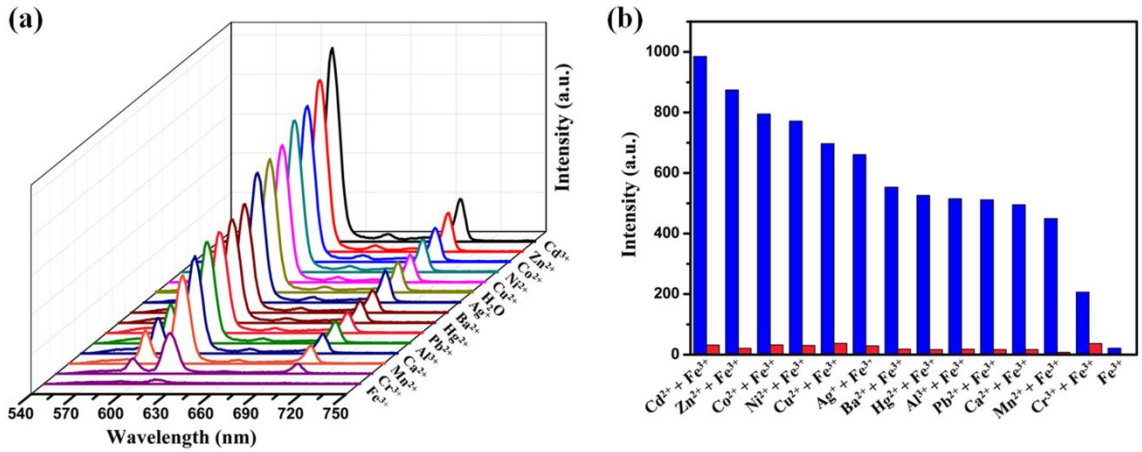

Fig. S13 (a) Luminescence spectra of **1A** in water treated with different metal ions (1×10^{-2} mol L^{-1}). (b) The luminescence intensities of **1A** at 616 nm upon the addition of different metal ions followed by Fe^{3+} ions. The blue bars represent the intensities in different metal ion aqueous solutions, the red bars represent the intensities in the mixed solutions of Fe^{3+} and other metal ions.

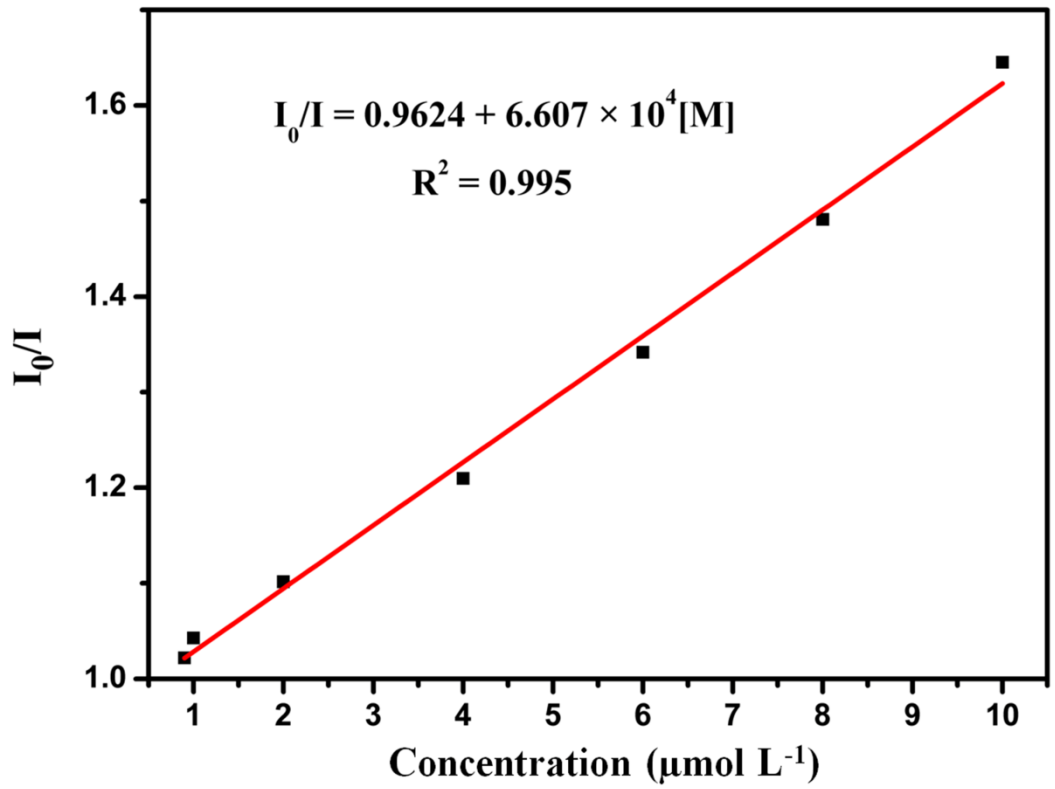

Fig. S14 The SV quenching curve for **1A** in aqueous solutions of different concentrations of Fe^{3+}.

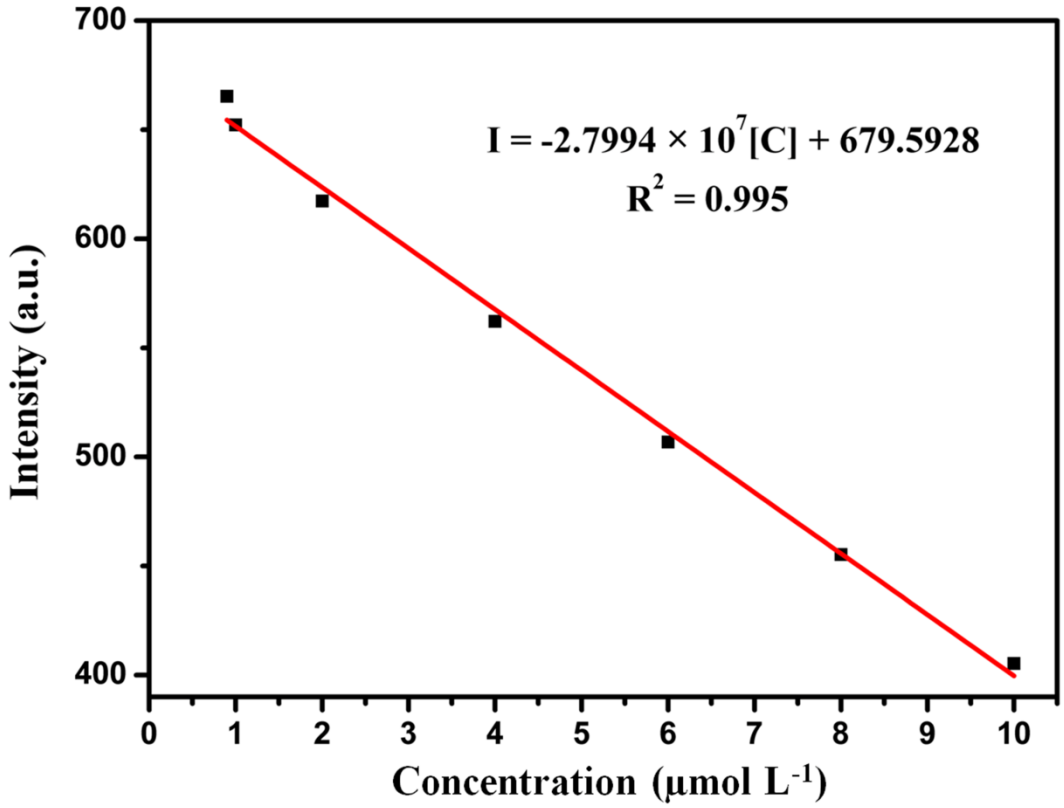

Fig. S15 Relation of luminescence intensity against Fe^{3+} added into **1A** suspension and their linear fitting curve for the estimation of LOD.

Detection Limit = $3\sigma/k$

= $(3 \times 8.1379)/ 2.7994 \times 10^7$ L mol^{-1}

= 0.87 µmol L^{-1}

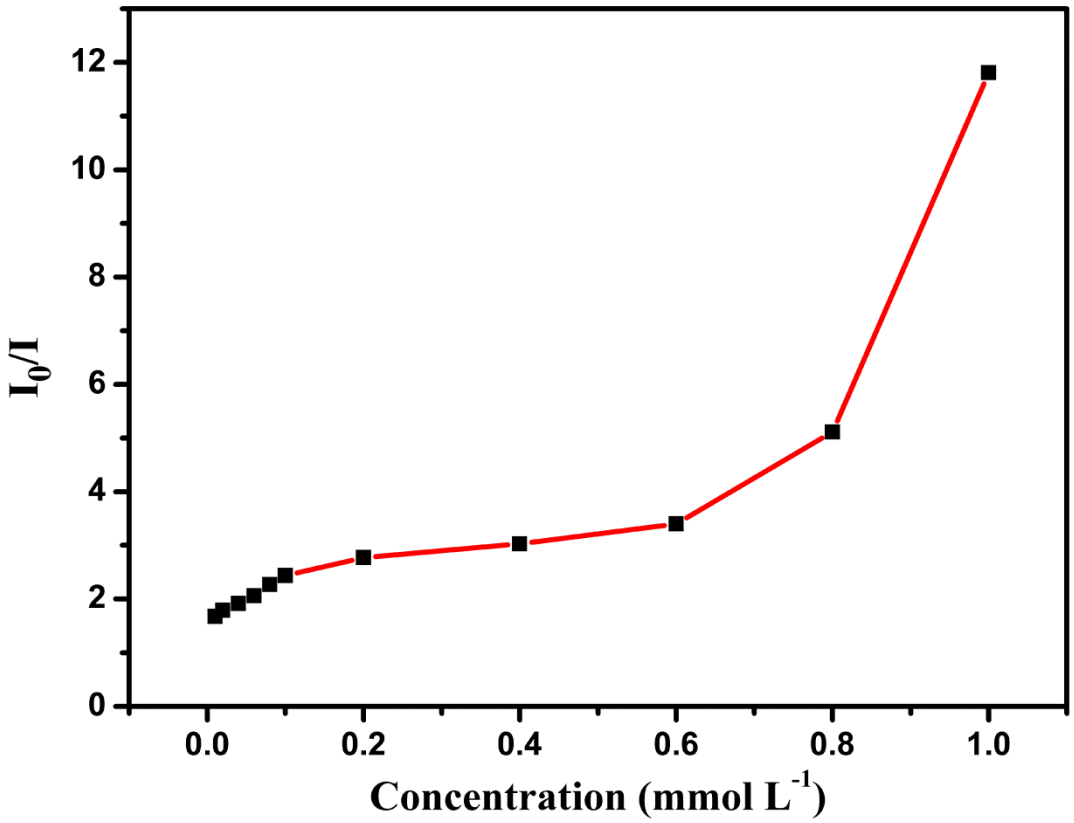

Fig. S16 Stern–Völmer plot for the luminescence intensities of **1A** in aqueous solutions of different concentrations of Fe^{3+}.

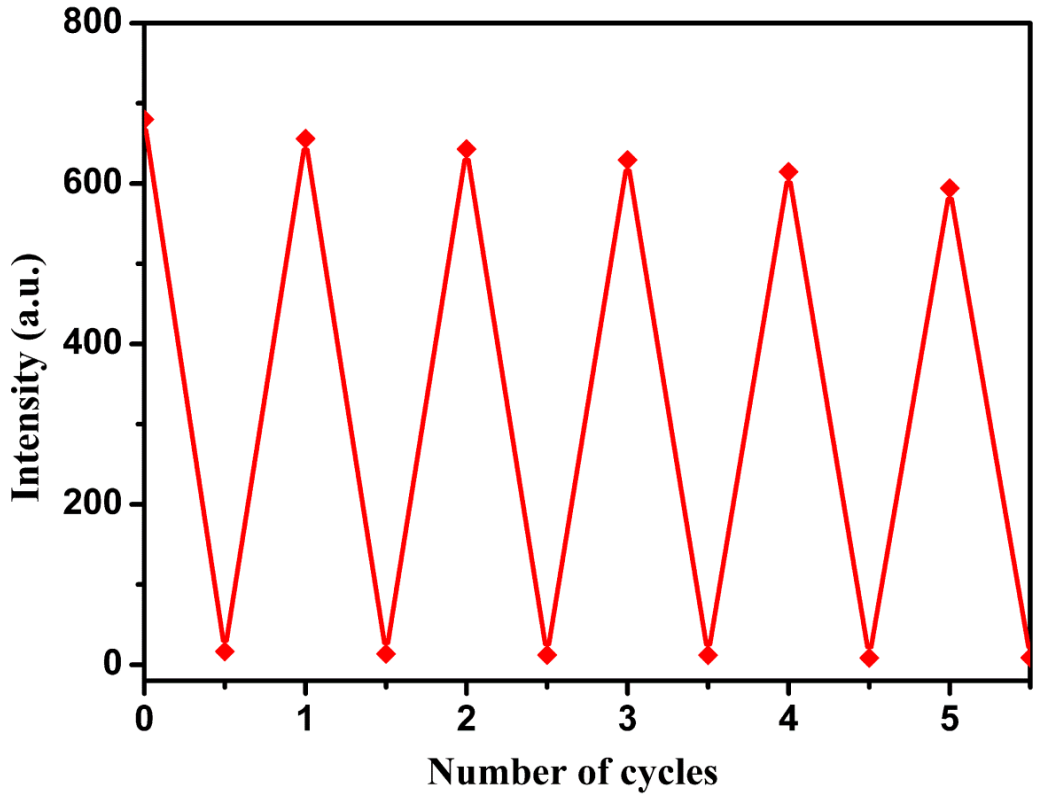

Fig. S17 Cyclic response of **1A** for detecting Fe^{3+} (luminescence intensity at 616 nm).

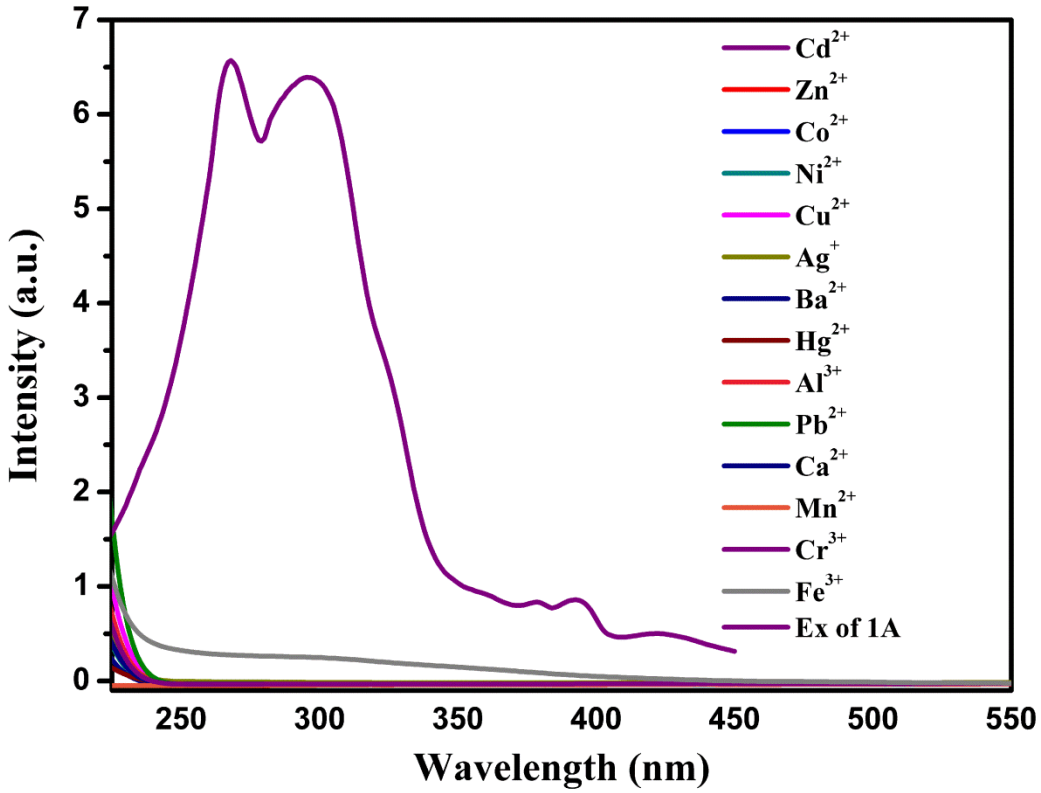

Fig. S18 The absorption spectra of various cations and the excitation spectrum of **1A**.

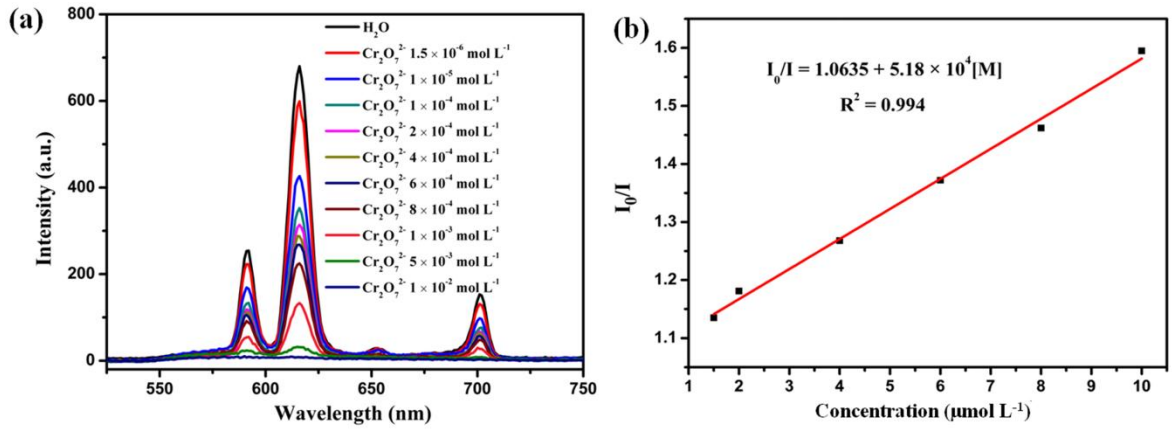

Fig. S19 (a) Luminescence spectra of **1A** in aqueous solutions containing different concentrations of $Cr_2O_7^{2-}$. (b) The SV quenching curve for **1A** in aqueous solutions of different concentrations of $Cr_2O_7^{2-}$.

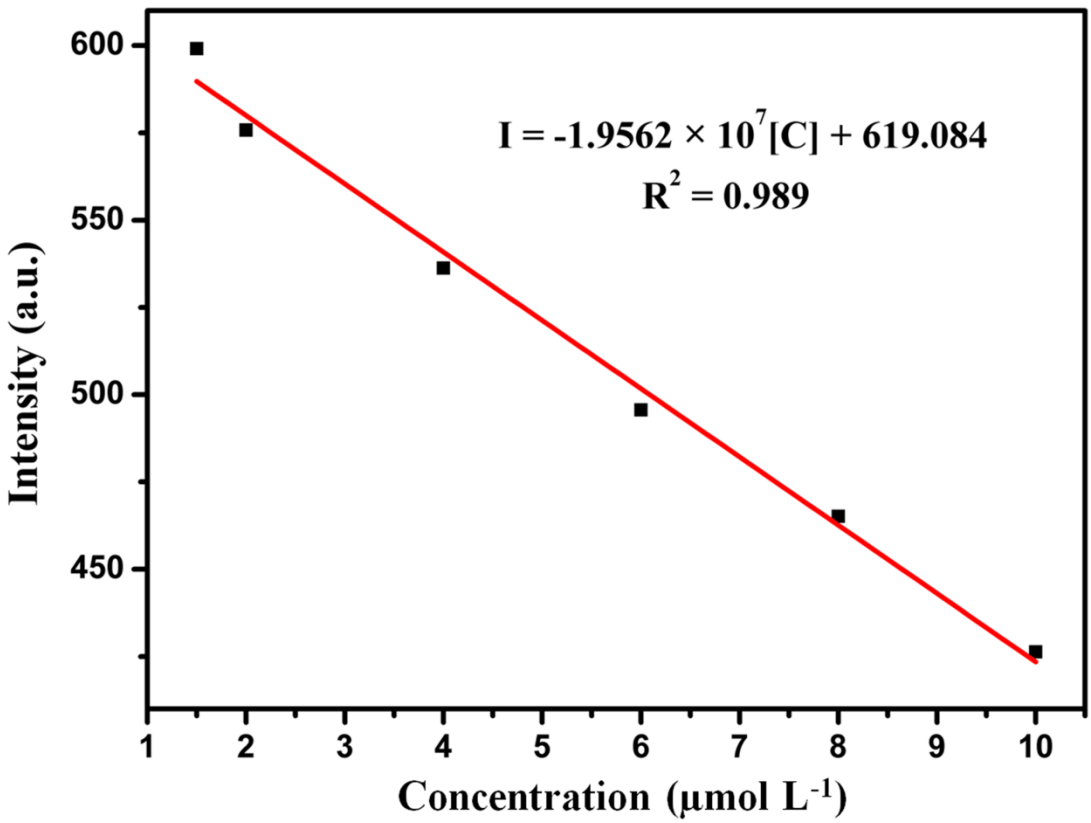

Fig. S20 Relation of luminescence intensity against $Cr_2O_7^{2-}$ added into **1A** suspension and their linear fitting curve for the estimation of LOD.

Detection Limit = 3σ/*k*

= (3 × 8.1379) / 1.9562 × 10^7 L mol^{-1}

= 1.25 µmol L^{-1}

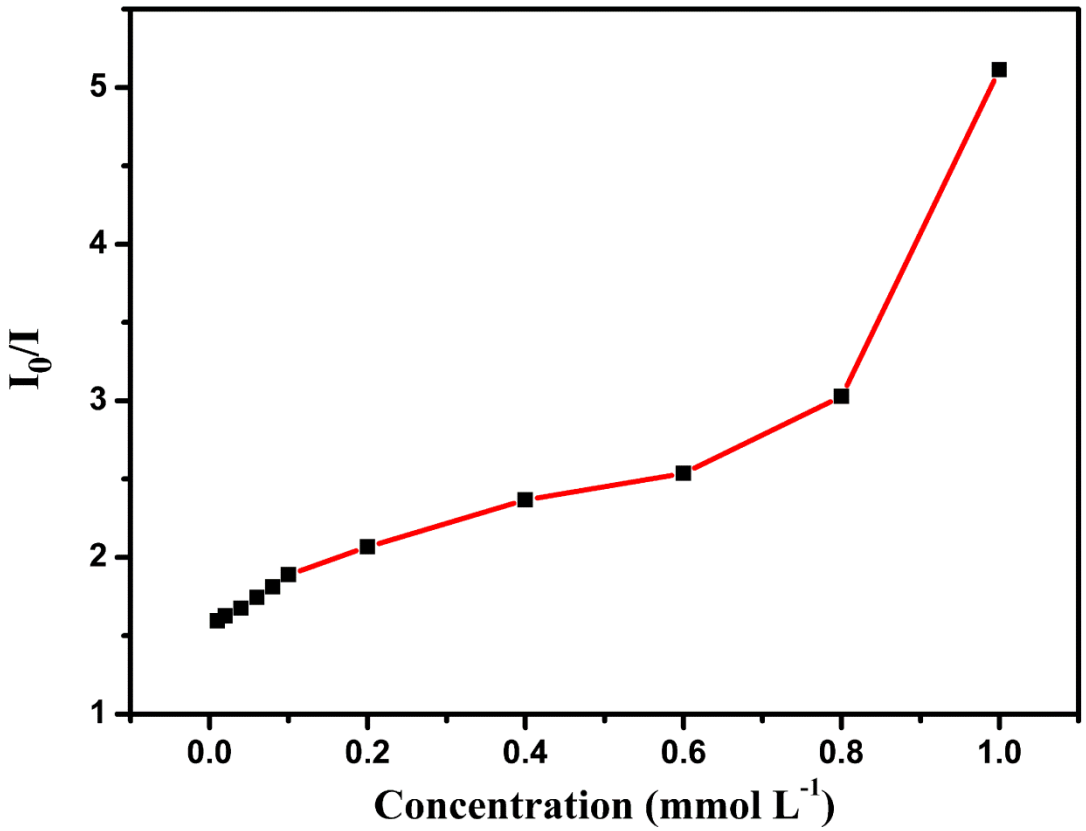

Fig. S21 Stern–Völmer plot for the luminescence intensities of **1A** in aqueous solutions of different concentrations of $Cr_2O_7^{2-}$.

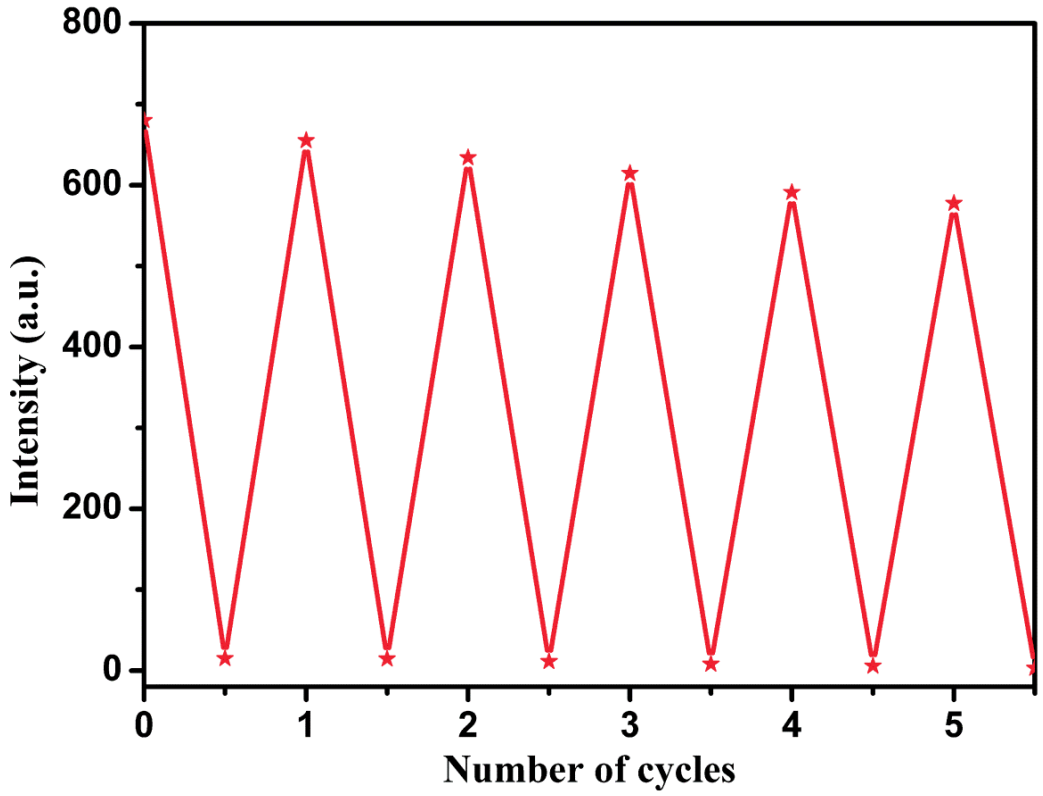

Fig. S22 Cyclic response of **1A** for detecting $Cr_2O_7^{2-}$ (luminescence intensity at 616 nm).

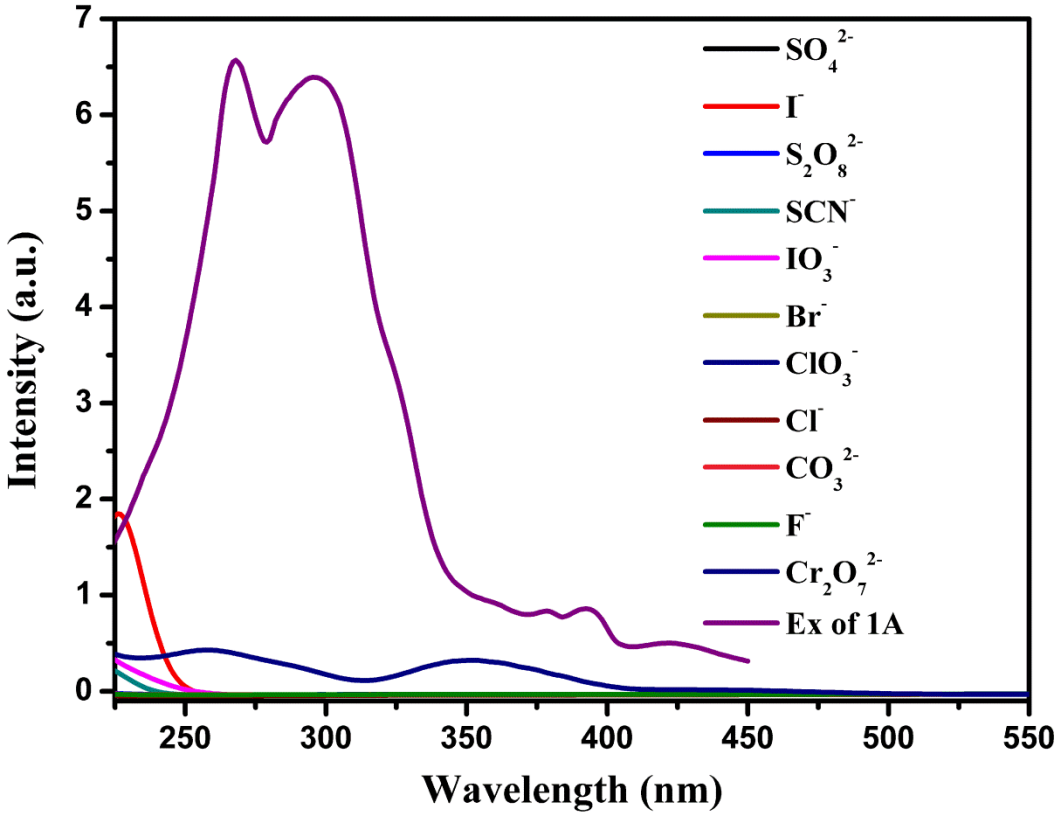

Fig. S23 The absorption spectra of various anions and the excitation spectrum of **1A**.

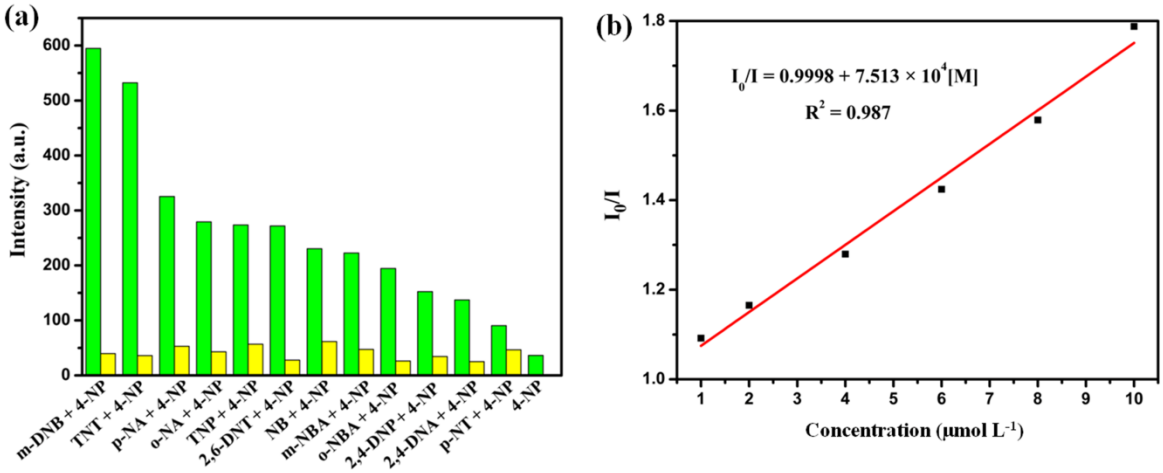

Fig. S24 (a) The luminescence intensities of **1A** at 616 nm upon the addition of different nitro explosives followed by 4-NP. The green bars represent the intensities in different nitro explosive aqueous solutions, the yellow bars represent the intensities in the mixed solutions of 4-NP and other nitro explosives. (b) The SV quenching curve for **1A** in aqueous solutions of different concentrations of 4-NP.

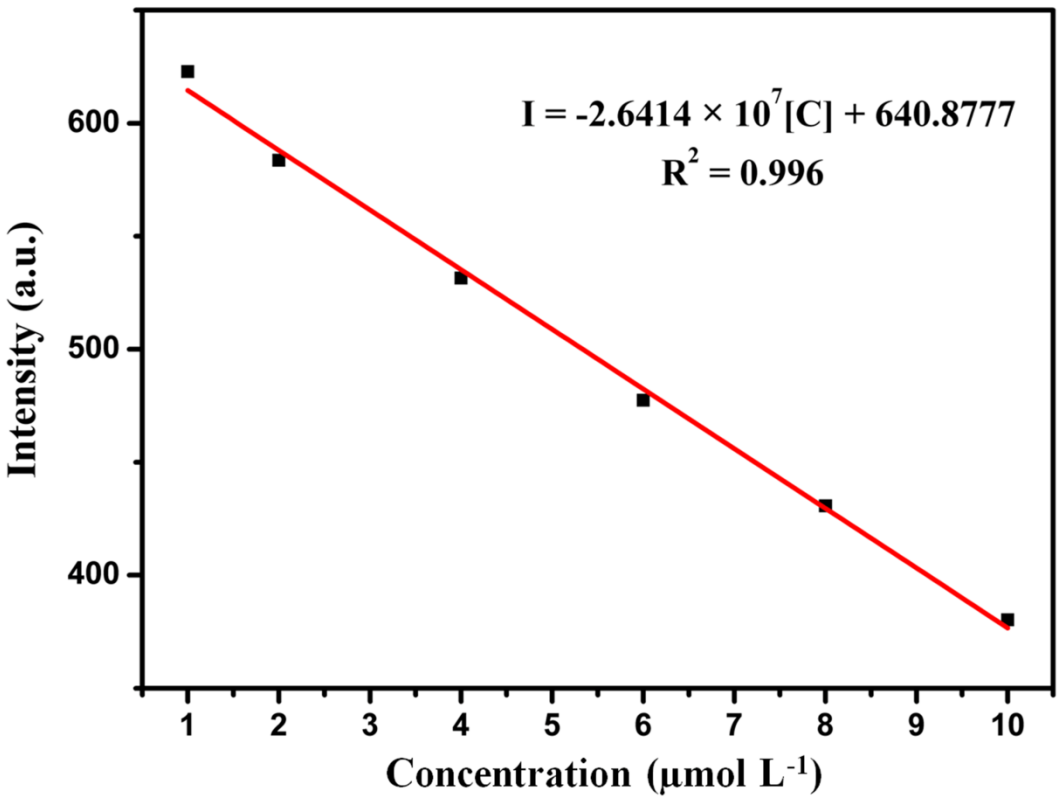

Fig. S25 Relation of luminescence intensity against 4-NP added into **1A** suspension and their linear fitting curve for the estimation of LOD.

Detection Limit = 3σ/*k*

= (3 × 8.1379) / 2.6414 × 10^7 L mol^{-1}

= 0.92 µmol L^{-1}

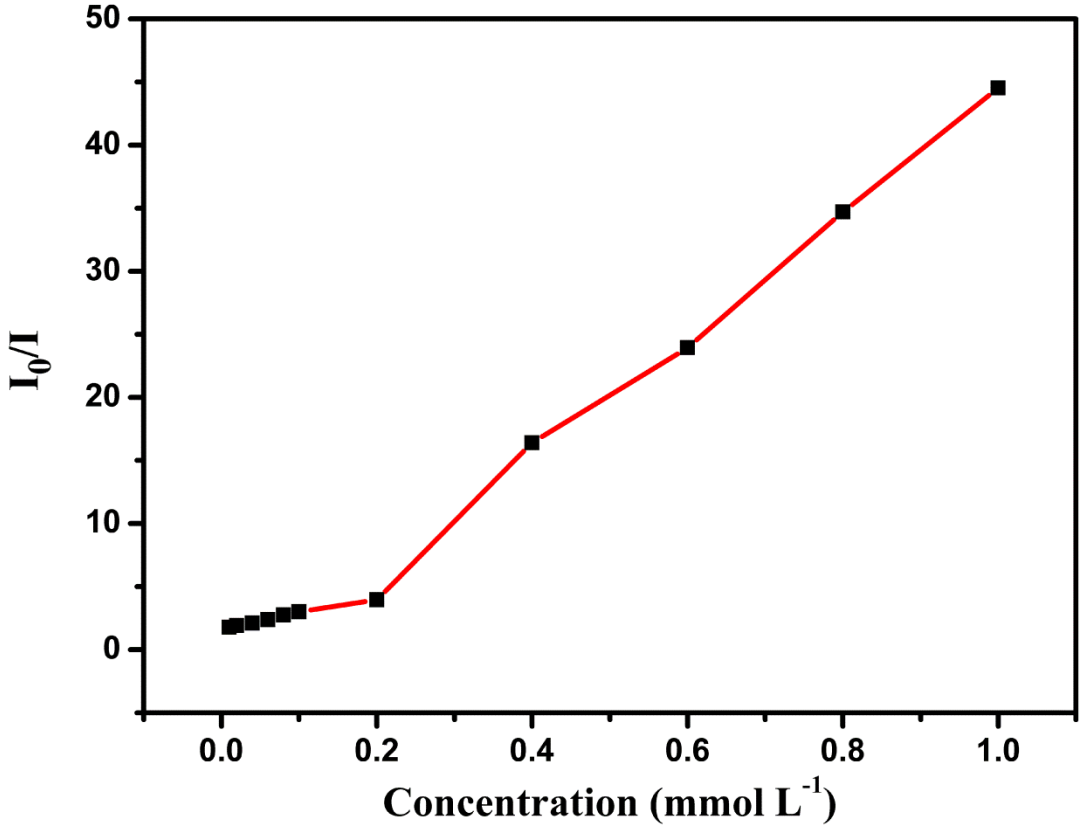

Fig. S26 Stern–Völmer plot for the luminescence intensities of **1A** in aqueous solutions of different concentrations of 4-NP.

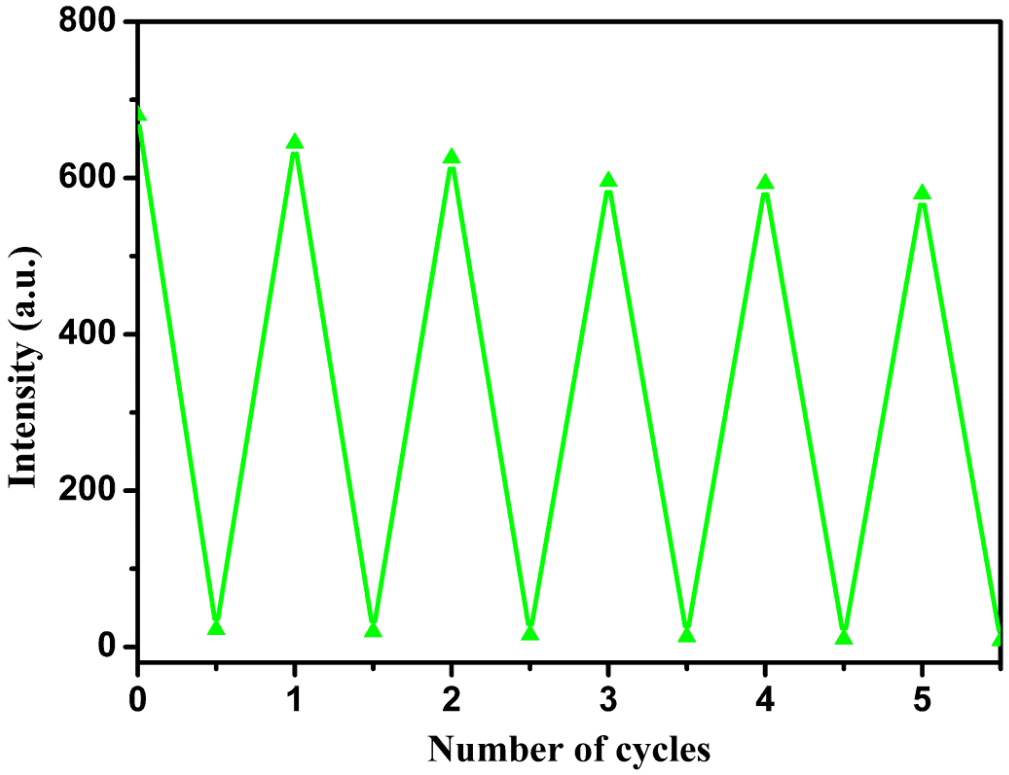

Fig. S27 Cyclic response of **1A** for detecting 4-NP (luminescence intensity at 616 nm).

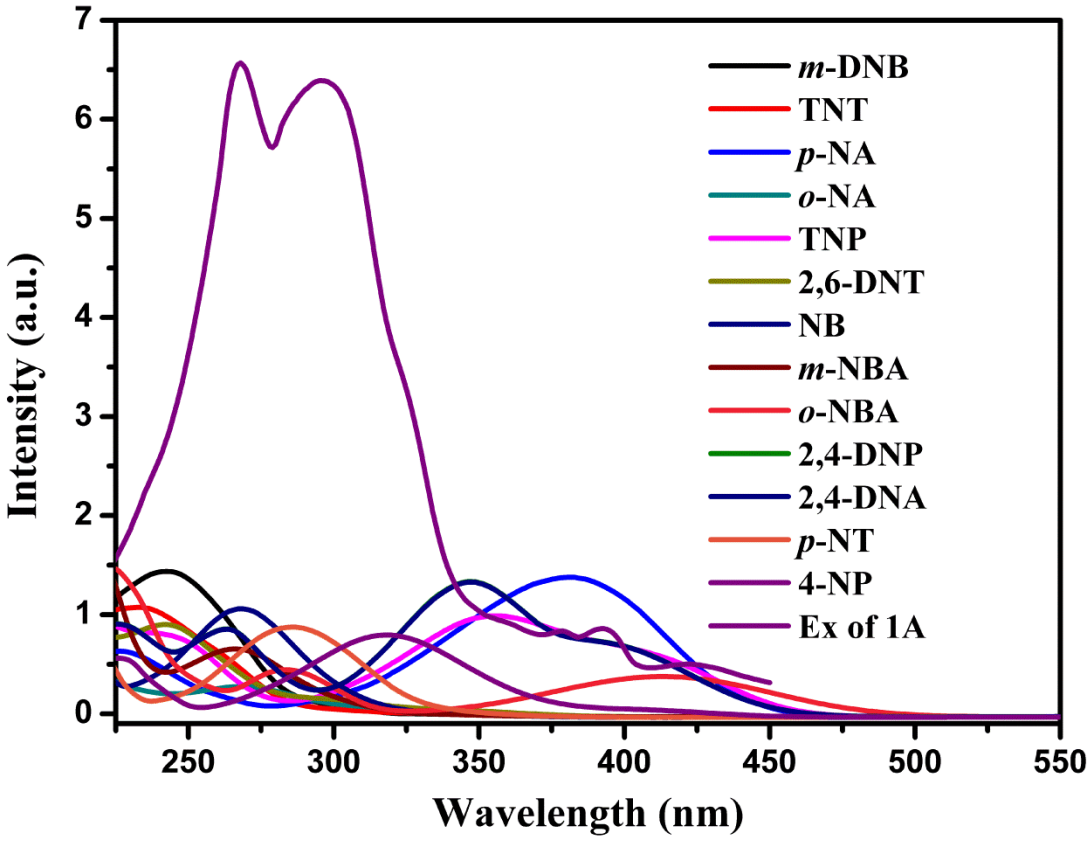

Fig. S28 The absorption spectra of different nitro explosives and the excitation spectrum of **1A**.

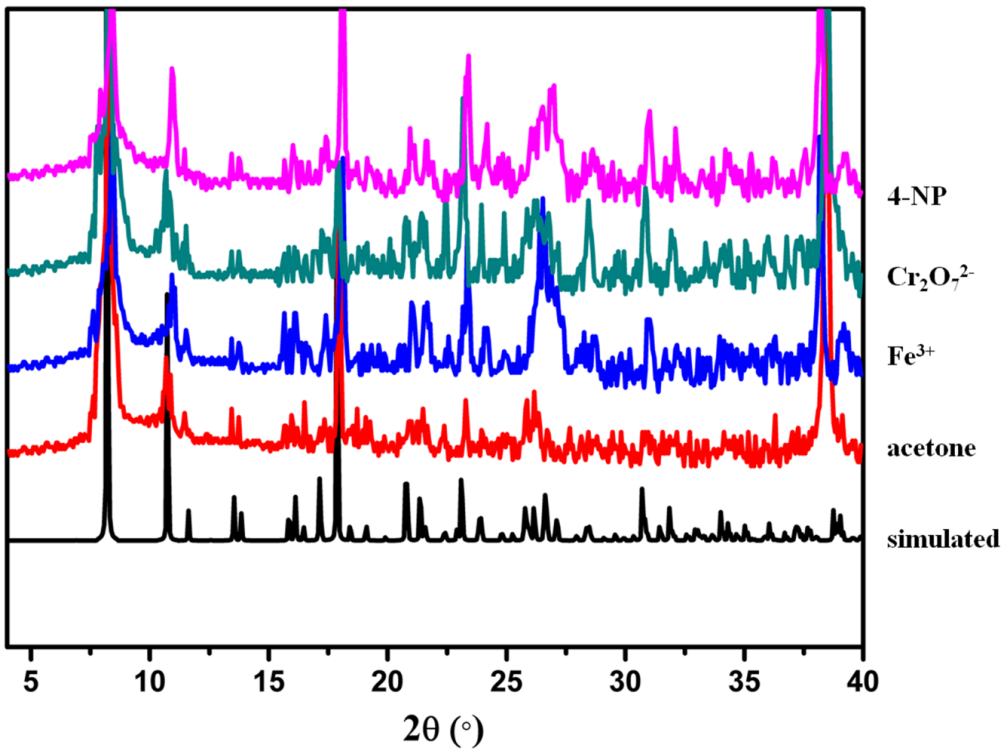

Fig. S29 The powder X-ray diffraction patterns of **1A** after cyclic sensing acetone, Fe^{3+}, $Cr_2O_7^{2-}$ and 4-NP in aqueous solutions.

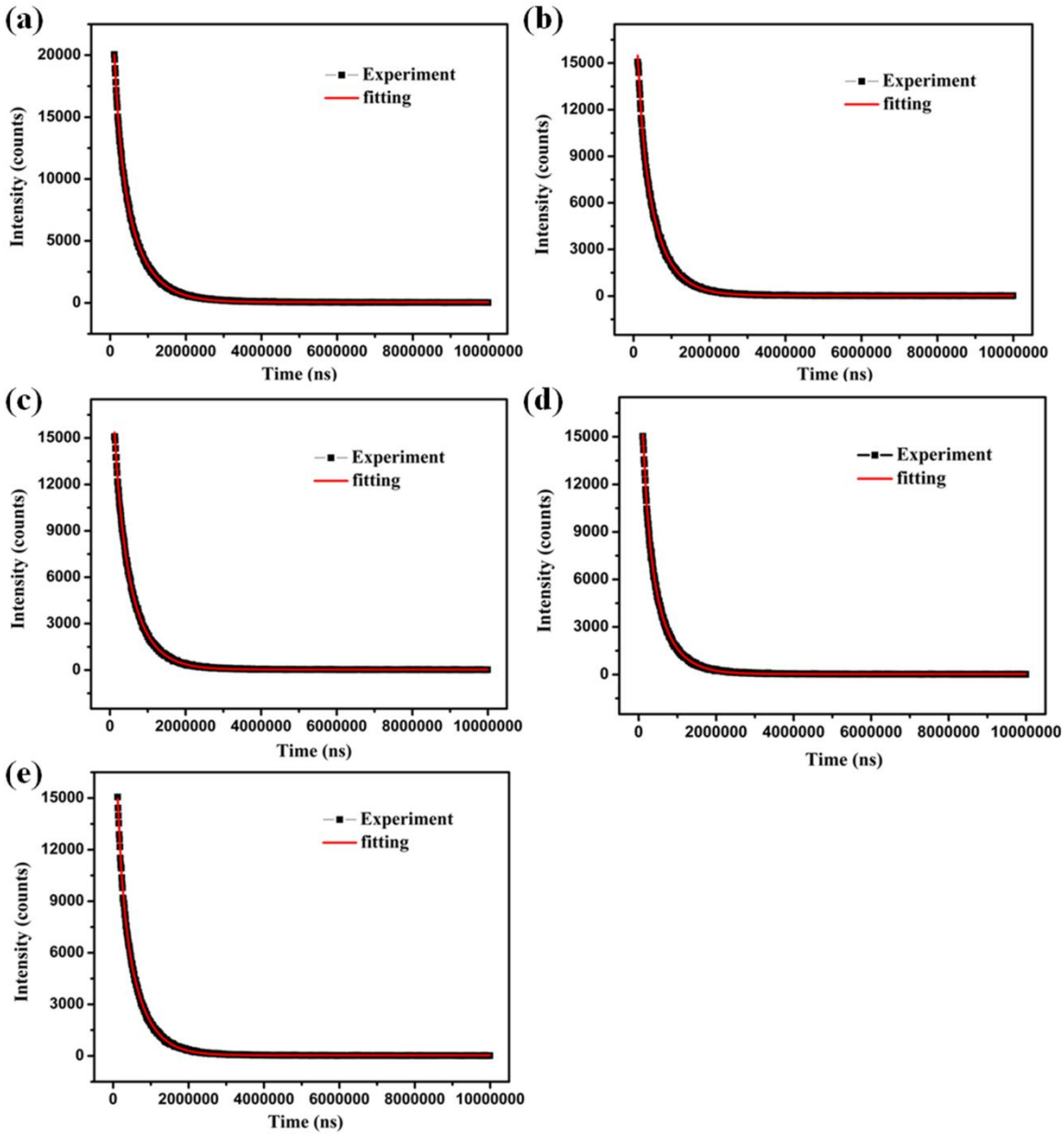

Fig. S30 Luminescence decay profiles for **1A** (a), acetone@**1A** (b), Fe^{3+}@**1A** (c), $Cr_2O_7^{2-}$@**1A** (d) and 4-NP@**1A** (e) recorded at room temperature. The $^5D_0$ decay curve of **1A** with emission was monitored at 614 nm (λ_{ex} = 328 nm). The red line is the best fitting to the data using a double exponential function, giving the value of τ_1 = 0.597 ms and τ_2 = 0.171 ms. The $^5D_0$ decay curve of acetone@**1A** with emission was monitored at 614 nm (λ_{ex} = 328 nm), τ_1 = 0.142 ms and τ_2 = 0.522 ms. The $^5D_0$ decay curve of Fe^{3+}@**1A** with emission was monitored at 614 nm (λ_{ex} = 328 nm), τ_1 = 0.535 ms and τ_2 = 0.198 ms. The $^5D_0$ decay curve of $Cr_2O_7^{2-}$@**1A** with emission was monitored at 614 nm (λ_{ex} = 328 nm), τ_1 = 0.496 ms and

τ_2 = 0.148 ms. The $^5D_0$ decay curve of 4-NP@**1A** with emission was monitored at 614 nm (λ_{ex} = 328 nm), τ_1 = 0.122 ms and τ_2 = 0.509 ms.

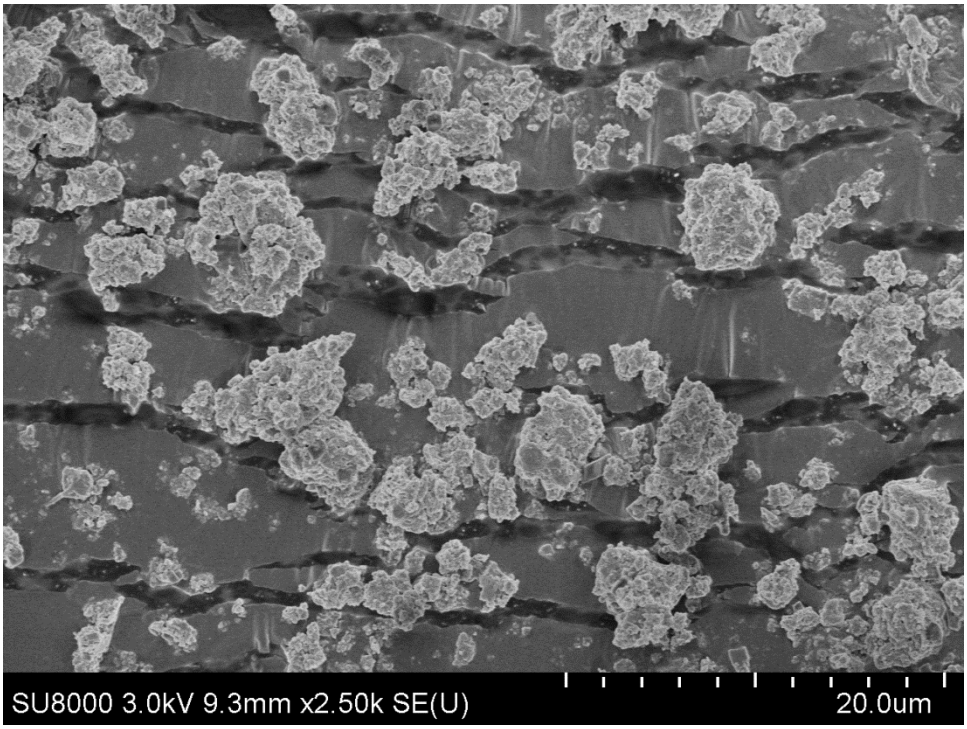

Fig. S31 SEM image of **1A** after grinding.

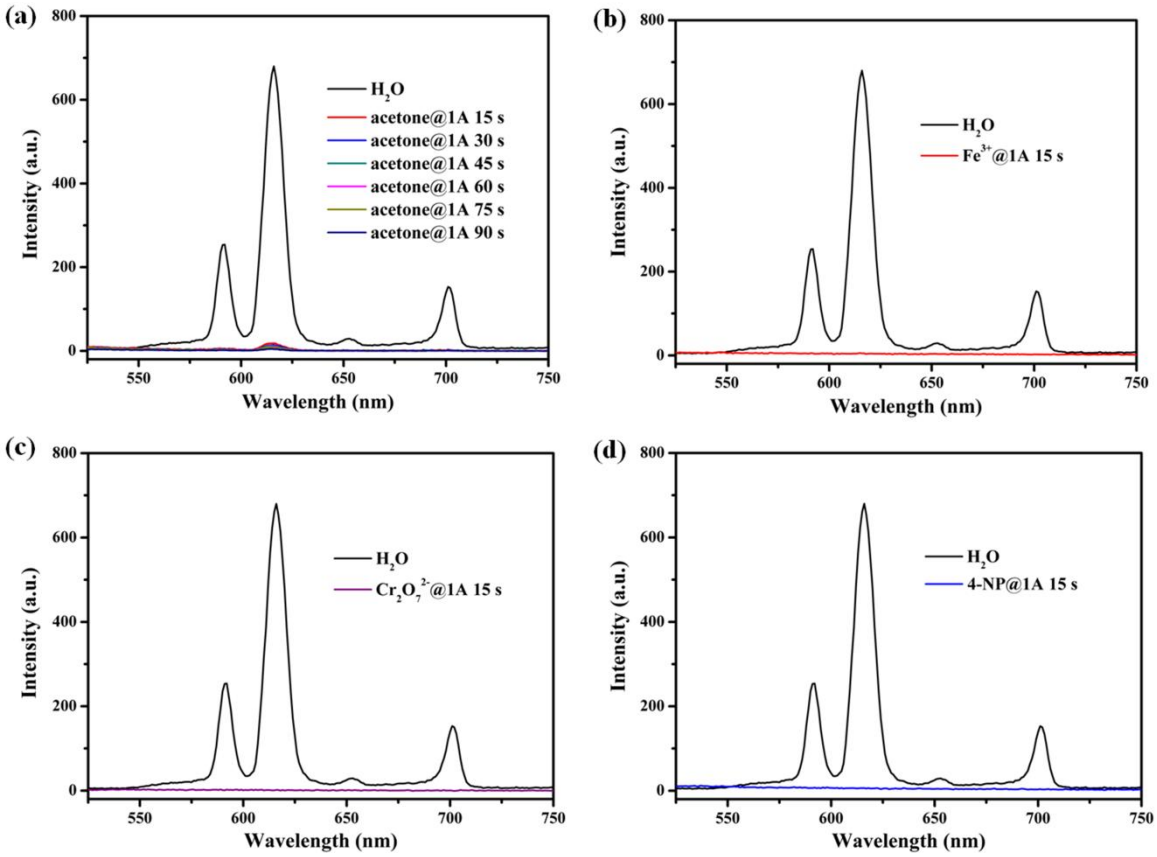

Fig. S32 Variation of luminescence intensity of **1A** with immersion time in analyte solution of acetone, $Fe(NO_3)_3$ (5×10^{-2} mol L^{-1}), $K_2Cr_2O_7^{2-}$ (1×10^{-2} mol L^{-1}) and 4-NP (1×10^{-3} mol L^{-1}), respectively.

Table S1. Luminescence lifetimes of **1A**, acetone@**1A**, Fe^{3+}@**1A,** $Cr_2O_7^{2-}$@**1A** and 4-NP@**1A**

Compounds	luminescence lifetimes (τ_{Eu3+})	
1A	τ_1 = 0.597 ms	τ_2 = 0.171 ms
acetone@**1A**	τ_1 = 0.142 ms	τ_2 = 0.522 ms
Fe^{3+}@**1A**	τ_1 = 0.535 ms	τ_2 = 0.198 ms
$Cr_2O_7^{2-}$@**1A**	τ_1 = 0.496 ms	τ_2 = 0.148 ms
4-NP@**1A**	τ_1 = 0.122 ms	τ_2 = 0.509 ms

Table S2. Crystal data and structure refinement for **1**

	1
Formula	$C_{16}H_{14}O_{9.5}Eu$
Fw (g mol^{-1})	528
Crystal system	Tetragonal
Space group	$I4_1/a$
a (Å)	21.534(3)
c (Å)	15.908(3)
V (Å^3)	7377(2)
Z	16
D_{Calc} (g cm^{-3})	1.758
μ (mm^{-1})	3.444
F (000)	3696
θ *range* (°)	3.11 - 27.47
Limiting indices	$-25 \leq h \leq 27$ $-27 \leq k \leq 27$ $-20 \leq l \leq 20$
Refl.Collected / unique	32891 / 4211
R_{int}	0.0412
Data / restraints / parameters	4211 / 0 / 226
GOF	1.074
R_1 [$I > 2\sigma(I)$]	0.0611
wR_2[$I > 2\sigma(I)$]	0.1910
R_1 (all data)	0.0657

wR_2 (all data)	0.1927
Largest diff.peak and hole(e $Å^{-3}$)	7.109 and -0.762
CCDC No.	1845244

Table S3. Selected bond lengths [Å] and angles [°] for **1**.

Eu(1)-O(8)#1	2.323(8)	Eu(1)-O(2)	2.461(10)
Eu(1)-O(6)#2	2.322(7)	O(3)-Eu(1)#5	2.359(7)
Eu(1)-O(7)#3	2.324(7)	O(5)-Eu(1)#6	2.331(7)
Eu(1)-O(5)#4	2.331(7)	O(6)-Eu(1)#7	2.322(7)
Eu(1)-O(1)	2.347(6)	O(7)-Eu(1)#8	2.324(7)
Eu(1)-O(3)#5	2.359(7)	O(8)-Eu(1)#9	2.323(8)
O(8)#1-Eu(1)-O(6)#2	91.4(3)	O(8)#1-Eu(1)-O(7)#3	71.8(3)
O(6)#2-Eu(1)-O(7)#3	91.8(3)	O(8)#1-Eu(1)-O(5)#4	71.7(3)
O(6)#2-Eu(1)-O(5)#4	98.9(3)	O(7)#3-Eu(1)-O(5)#4	142.1(3)
O(8)#1-Eu(1)-O(1)	105.4(3)	O(6)#2-Eu(1)-O(1)	162.6(3)
O(7)#3-Eu(1)-O(1)	89.4(3)	O(5)#4-Eu(1)-O(1)	90.6(3)
O(8)#1-Eu(1)-O(3)#5	147.3(3)	O(6)#2-Eu(1)-O(3)#5	87.9(3)
O(7)#3-Eu(1)-O(3)#5	140.9(3)	O(5)#4-Eu(1)-O(3)#5	76.2(3)
O(1)-Eu(1)-O(3)#5	80.3(3)	O(8)#1-Eu(1)-O(2)	140.5(4)
O(6)#2-Eu(1)-O(2)	84.4(4)	O(7)#3-Eu(1)-O(2)	69.1(4)
O(5)#4-Eu(1)-O(2)	147.8(4)	O(1)-Eu(1)-O(2)	79.8(4)
O(3)#5-Eu(1)-O(2)	71.9(4)	C(3)-O(1)-Eu(1)	122.3(6)
C(1)-O(3)-Eu(1)#5	141.6(7)	C(3)-O(5)-Eu(1)#6	165.1(7)
C(12)-O(6)-Eu(1)#7	131.9(7)	C(1)-O(7)-Eu(1)#8	158.7(7)
C(12)-O(8)-Eu(1)#9	163.9(8)		

Symmetry transformations used to generate equivalent atoms:

#1 y-3/4, -x+5/4, z-3/4; #2 x, y, z-1; #3 -y+3/4, x+3/4, -z+3/4; #4 –y+5/4, x+3/4, z-1/4; #5 -x+1/2, -y+3/2, -z+1/2; #6 y-3/4, -x+5/4, z+1/4; #7 x, y, z+1; #8 y-3/4, -x+3/4, -z+3/4; #9 –y+5/4, x+3/4, z+3/4.

Table S4. The comparison of K_{SV} between **1A** and other reported luminescent sensors for the detection of acetone.

MOFs	K_{SV}	Detection limits (vol%)	Reference
$[Eu(L)(H_2O)]\cdot 2.5H_2O$	0.7019	0.0704	This work
$[Eu(BTB)(H_2O)_2 \text{ solvent}]_n$	42.6	0.3	22
$[Cd(Tipb)(pta)_{0.5}(H_2O)\text{-}(NO_3)]\cdot(DMF)x(H_2O)_y$	-	0.084	[1]
$[Cd(Tipb)(mta)]\cdot(DMF)_x(H_2O)_y$	-	0.075	[1]
$Cd_3(L)(H_2O)_2(DMF)_2\cdot 5DMF$	-	0.1	[2]
$Cd_3(L)(dib)\cdot 3H_2O\cdot 5DMA$	-	0.1	[2]
$Eu(BTC)(H_2O)\cdot 1.5H_2O$	-	0.3	[3]
$Tb(BTC)(H_2O)_6$	-	0.3	[4]

Table S5. The comparison of K_{SV} between **1A** and other reported luminescent sensors for the detection of Fe^{3+} ions.

MOFs	K_{SV} (L mol^{-1})	Detection limits (μmol L^{-1})	Reference
$[Eu(L)(H_2O)]\cdot 2.5H_2O$	6.607×10^4	0.87	This work
$[Zn(H_2bptc)(2,2'\text{-bipy})(H_2O)]\cdot 3H_2O$	2.581×10^4	9.5	[5]
$[Zn_2(bptc)(H_2O)]\cdot(4,4'\text{-bipy})_{0.5}$	2.826×10^4	8.5	[5]
$\{[Eu_2L_{1.5}(H_2O)_2EtOH]\cdot DMF\}_n$	2.94×10^3	10	[6]
EuL_3	4.1×10^3	-	[7]
534-MOF-Tb	5.51×10^3	-	[8]
Pb_3O_2L	7.80×10^3	7.85	4a
$\{[Cd(L)\text{-}(BPDC)]\cdot 2H_2O\}_n$	3.64×10^4	2.21	[9]
$\{[Cd(L)(SDBA)(H_2O)]\cdot 0.5H_2O\}_n$	3.59×10^4	7.14	[9]

Table S6. The comparison of K_{SV} between **1A** and other reported luminescent sensors for the detection of $Cr_2O_7^{2-}$ ions.

MOFs	K_{SV} (L mol^{-1})	Detection limits (μmol L^{-1})	Reference
[Eu(L)(H_2O)] 2.5H_2O	5.18 × 10^4	1.25	This work
{[Tb(TATAB)(H_2O)$_2$] NMP H_2O}$_n$	1.11 × 10^4	5	41
[Eu_2(tpbpc)$_4$ CO_3 4H_2O] DMF solvent	1.04 × 10^4	3.64	3a
{[$Eu_2L_{1.5}$(H_2O)$_2$EtOH] DMF}$_n$	1.526 × 10^3	10	[6]
Eu^{3+}@MIL-121	4.34 ×10^3	-	[10]
534-MOF-Tb	1.37 × 10^4	140	[8]
[Zn_2(TPOM)(NH_2-BDC)$_2$] 4H_2O	7.59 × 10^3	3.9	[11]
{[Cd(L)-(BPDC)] 2H_2O}$_n$	6.4 × 10^3	37.6	[9]
{[Cd(L)(SDBA)(H_2O)] 0.5H_2O}$_n$	4.96 × 10^3	48.6	[9]

Table S7. The comparison of K_{SV} between **1A** and other reported luminescent sensors for the detection of 4-NP.

MOFs	K_{SV} (L mol^{-1})	Detection limits (μmol L^{-1})	Reference
[Eu(L)(H_2O)] ·2.5H_2O	7.513 × 10^4	0.92	This work
Pb_3O_2L	3.31 × 10^3	2.16	4a
Zn-MOF-1	1.25 × 10^4	3.74	[12]
[Zn_2(TPOM)(NH_2-BDC)$_2$] ·4H_2O	2.17 × 10^4	3.5	[11]
[Gd_6(L)$_3$(HL)$_2$(H_2O)$_{10}$] ·18H_2O ×(solvent)	8.4 × 10^3	12	[13]
[Eu_6(L)$_3$(HL)$_2$-(H_2O)$_{10}$] ·10H_2O ×(solvent)	-	1.7	[14]

References

[1] Y. Li, H. Song, Q. Chen, K. Liu, F.-Y. Zhao, W.-J. Ruan and Z. Chang, *J. Mater. Chem. A*, 2014, **2**, 9469–9473.

[2] F.-Y. Yi, W.-T. Yang and Z.-M. Sun, *J. Mater. Chem.*, 2012, **22**, 23201–23209.

[3] B. Chen, Y. Yang, F. Zapata, G. Lin, G. Qian and E. B. Lobkovsky, *Adv. Mater.*, 2007, **19**, 1693–1696.

[4] W. T. Yang, J. Feng and H. J. Zhang, *J. Mater. Chem.*, 2012, **22**, 6819–6823.

[5] J. Sun, P. Zhang, H. Qi, J. Jia, X. D. Chen, S. B. Jing, L. Wang and Y. Fan, *Inorganica Chimica Acta*, 2018, **469**, 298–305.

[6] W. Liu, X. Huang, C. Xu, C. Y. Chen, L. Z. Yang, W. Dou, W. M. Chen, H. Yang and W. S. Liu, *Chem. – Eur. J.*, 2016, **22**, 18769 –18776.

[7] M. Zheng, H. Q. Tan, Z. G. Xie, L. G. Zhang, X. B. Jing and Z. C. Sun, *ACS Appl. Mater. Interfaces*, 2013, **5**, 1078–1083.

[8] M. Chen, W.-M. Xu, J.-Y. Tian, H. Cui, J.-X. Zhang, C.-S. Liu and M. Du, *J. Mater. Chem. C*, 2017, **5**, 2015–2021.

[9] S. G. Chen, Z. Z. Shi, L. Qin, H. L. Jia and H. G. Zheng, *Cryst. Growth Des.*, 2017, **17**, 67–72.

[10] J.-N. Hao and B. Yan, *New J. Chem.*, 2016, **40**, 4654–4661.

[11] R. Lv, J. Y. Wang, Y. P. Zhang, H. Li, L. Y. Yang, S. Y. Liao, W. Gu and X. Liu, *J. Mater. Chem. A*, 2016, **4**, 15494–15500.

[12] X.-Y. Guo, F. Zhao, J.-J. Liu, Z.-L. Liu and Y.-Q. Wang, *J. Mater. Chem. A*, 2017, **5**, 20035–20043.

[13] Q.-H. Tan, Y.-Q. Wang, X.-Y. Guo, H.-T. Liu and Z.-L. Liu, *RSC Adv.*, 2016, **6**, 61725–61731.

[14] Y.-Q. Wang, Q.-H. Tan, H.-T. Liu, W. Sun and Z.-L. Liu, *RSC Adv.*, 2015, **5**, 86614–86619.